bioresources.com

The Effect of Shrinkage Anisotropy on Tangential Rheological Properties of Asian White Birch Disks

Zongying Fu, Yingchun Cai,* Jingyao Zhao, and Siqi Huan

The process of wood drying can induce defects caused by drying stress, which limits the processing and utilization of this valuable material. Here, we investigated elastic strain, viscoelastic creep strain, and mechano-sorptive (MS) creep strain caused by shrinkage anisotropy using the image analytical method during slow conventional drying of white birch (*Betula platyphylla* Suk) disks. The rheological properties of wood disks with different moisture contents (MC) were analyzed together with the influences of MC and radial position on each strain. The results showed that relations between stress and strain are complex; below the fiber saturation point (FSP), the wood disk is initially subject to tangential tensile stress; with decreasing MC, the tensile stress turns into a compressive stress. MS creep strain increased with decreasing MC; however, elastic strain and viscoelastic creep strain were positively correlated with MC. Elastic strain decreased after first increasing, and then remained stable while the MS creep strain significantly increased from pith to bark, at 10% MC and 18% MC, respectively. Shrinkage anisotropy was the main reason for strain during the drying processing, and it was one of the main factors causing cracks during drying or application.

Keywords: White Birch disk; Shrinkage anisotropy; Elastic strain; Viscoelastic creep strain; MS creep strain

*Contact information: Key Laboratory of Bio-based Material Science and Technology of the Ministry of Education, Northeast Forestry University, 150040, Harbin; *Corresponding author: ychcai@aliyun.com*

INTRODUCTION

Drying stress is the main cause of material defects that develop during wood drying. The defects not only limit the normal processing and utilization of wood, but also increase the burden on gradually decreasing wood resources. Therefore, the mechanism of stress and strain development during wood drying has been a focus of study in the wood industry. Scholars have carried out research in this area for a long time (McMillen 1955a,b; Ugolev 1976; Hasalania and Itayaa 1996; Tu *et al.* 2007; Bergman 2010). Wood disks are an effective way to make use of bent wood and small-diameter wood. These materials are valuable as wood artifacts because of their inherent beauty, such as bowls and dials; waste during the sawing process usually occurs as lumber that is cut lengthwise rather than a cross section (Lee and Hayashi 2000). Research has not sufficiently addressed the problem that disk drying is more difficult, due to crack formation, than lumber drying.

With the development of wood physics, researchers have started to apply polymer rheology theory to the study of wood drying stress. At present, most researchers agree that the strain during wood drying comprises elastic strain, viscoelastic creep strain, mechano-sorptive (MS) creep strain, and free shrinkage strain. A better understanding of

the stress factors during wood drying will offer important parameters to explain wood cracks using rheological theory and ultimately improve the wood drying quality. After Armstrong (1960 and 1962) published the MS creep phenomenon of wood, more and more scholars began to focus on the rheological properties of wood. Leicester (1971) and Hunt (1989) believed that MS creep consisted of recoverable and irreversible parts. Rice and Youngs (1990) found that MS creep strain was the main strain when studying the relationship between MC and elastic strain, viscoelastic creep strain, and MS creep strain in the early drying stage of red oak. Erickson and Seavey (1992) noted that high-temperature drying treatment released drying stress and reduced the moisture gradient in the red oak drying process. Svensson (1995 and 1996) reported that temperature and MC were positively correlated with creep when drying Scots pine in the kiln drying process. Zhan *et al.* (2009) investigated the rheological properties of larch disks during a conventional drying process, noting that an increase in MS creep strain would benefit drying stress relaxation to a certain extent.

White birch is a fast-growing plantation species in northeast China; thirty-year-old birch trees can reach a height of 12 m and a diameter of 16 cm. Ai *et al.* (1996) and Wang *et al.* (1997) discussed the drying technology and characteristics of small diameter birch disks. Zhan *et al.* (2004) analyzed the transverse strains of white birch lumber through the rheology theory in drying process.

This study was undertaken to investigate the effects of shrinkage anisotropy on each strain during slow drying of birch disks. The influence of MC and radial position on each strain were also discussed. Decreasing the variability of MC across the wood during the drying process has been unsuccessfully used as a method to reduce cracks. It is evident that shrinkage anisotropy has an important impact on stress and crack development, but there have been no reports on the mechanisms by which this occurs. Separate measurement and analysis of the strain caused by shrinkage anisotropy were used to prepare for a follow-up study into the mechanisms of the combined action by MC gradient and shrinkage anisotropy.

EXPERIMENTAL

Materials

Twenty-two-year-old plantation white birch trees with an average diameter of 23 cm were obtained from forests in the region of the Lesser Khingan Mountains, located in the Heilongjiang Province, China. The initial MC of the wood was more than 60%. The logs were sawn into several wood disks of 30-mm thickness at a distance of 0.3 m from the roots, numbered, and stored in a freezer to keep them in green condition. Ten wood disks without obvious defects were selected from one birch trunk, with an average diameter of about 22 cm, of which one specimen was used to determine the green MC, three specimens were used to ensure the target MC (26%, 18%, and 10%), and the remaining six samples were divided into three groups for strain studies at each target MC.

Method

The experiments were conducted in a GDS-100 conditioning chamber. At a constant temperature of 40 °C, the relative humidity decreased slowly, as shown in Fig. 1. The hygrometric difference increased slowly and was balanced for 6 h at intervals of 12 h to ensure that the internal MC in the timber was distributed evenly, eliminating

drying stress caused by uneven MC distribution and only considering drying stress generated by shrinkage anisotropy. The sawn surface of the samples was polished and lined with a grid, as shown in Fig. 2. Strain slices of the following dimensions were cut along the grid lines during the drying process at MCs of 26%, 18%, and 10%: 30 mm (tangential) $\times$ 10 mm (radial)$\times$ 30 mm (longitudinal). Each strain was measured at a given MC using the image analytical method . The image analytical method employed here is an image-based, non-contact method that measures dot pitch. Consecutive images of the samples are collected together with a ruler during the drying process at different MCs by high-resolution digital equipment. The images are subsequently imported into ImageJ imaging software to measure and analyze the actual length of the grid on the samples.
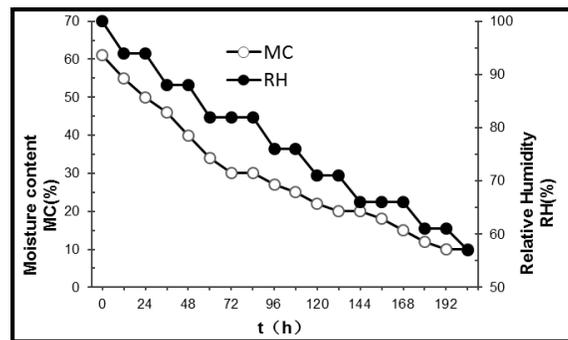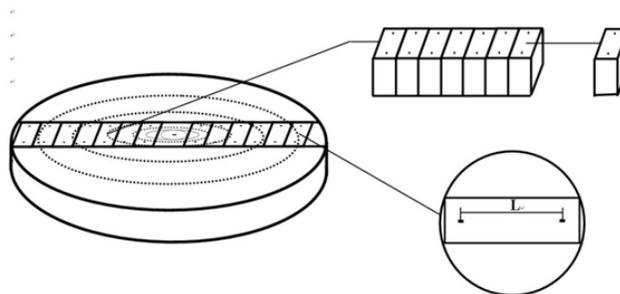
Fig. 1. Drying schedule

Fig. 2. Diagram of the cutting of strain slices

The size of strain slices at different states during drying

Figure 3 shows a cutting diagram of the strain slices based on previous studies (Rice and Youngs 1990; Li and Gu 1999; Zhan *et al*. 2009).

L_0—Distance between two measuring points on the strain slices under green conditions.

L_1—Distance between two measuring points on the strain slices before cutting at MCs of 26%, 18%, and 10%.

L_2—Distance between two measuring points on the strain slices when the wood disk is split along the grid line.

L_3—Distance between two measuring points under stable moisture conditions, achieved by placing the strain slices in a conditioning chamber with EMC equal to MC when the slice is split.

L_4—Distance between two measuring points with the strain slices soaked in water for 24 h, steamed for 10 h, and placed in a conditioning chamber to maintain the temperature and humidity conditions in L_3.

The strain slices were bundled together with elastic before acquiring images L_2, L_3, L_4, and they were placed in a conditioning chamber to prevent warp and deformation.
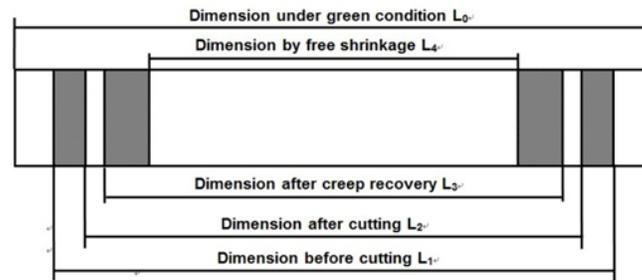

Fig. 3. The size of the strain slice at different drying states

The strains and calculations

Elastic strain: $\varepsilon_E = (L_2 - L_1)/L_0$ (1)

Viscoelastic creep strain: $\varepsilon_V = (L_3 - L_2)/L_0$ (2)

MS creep strain: $\varepsilon_M = (L_4 - L_3)/L_0$ (3)

THE ANALYSIS OF STRESSES IN WOOD DISKS DURING DRYING

Below the FSP, the wood disk begins to shrink due to the loss of bound water. Due to the difference between the tangential and radial shrinkage (in general, tangential shrinkage is twice that of radial shrinkage), tangential shrinkage is limited by radial shrinkage. For wood disks, the acting force has a radial distribution from pith to bark and forms a circle around the wood disk (unit torus acting force *f1*). In addition, tangential strain in each layer caused by shrinkage anisotropy is positively correlated with the radius and the difference in the free shrinkage ratio between the tangential and radial directions (Yang 2011). Therefore, each layer is subject to micro pressure by the outer layer adjacent to it (unit torus pressure *f2*). A tangential microelement was randomly selected from the wood disk as the object of this study. The forces are shown in Fig. 4(a), where *F1* and *F2* are the respective resultant forces of *f1* and *f2*, which are applied to the microelement. T_1 and T_2 are the tangential tensile stresses of the areas next to the microelement in the same layer. The resultant force of T_1 and T_2 is balanced with *F*, which is the resultant force of *F1* and *F2*.

During stage 4(a), elastic strain appeared under two tangential stresses for the microelement, while viscoelastic creep strain emerged with increasing time. Once the tangential stress exceeded the proportional limit, plastic deformation occurred. When it exceeded the tangential tensile strength, the wood cracked as a result (Kang and Lee 2004). The tensile plastic deformation restrains tangential shrinkage, while it has no influence on radial shrinkage. In cases when the tangential shrinkage occurs at the same

rate as the radial shrinkage, shrinkage does not create any internal stress. With the development of plastic deformation, when the radial shrinkage rate is higher than the tangential shrinkage rate, stress reversal begins to happen, and each layer is subjected to a radial tensile force (unit torus acting force *f1*). Meanwhile, because the tensile strain and tensile plastic deformation in the outer layer are greater than that in the adjacent inner layer, each layer is subject to micro tension by the outer layer adjacent to it. The analysis of forces on the microelement is shown in Fig. 4(b), where *F1* and *F2* are the respective resultant forces of *f1* and *f2*, which are applied to the microelement. T_1 and T_2 are the tangential compressive stresses of the areas next to the microelement in the same layer. The resultant force of T_1 and T_2 is balanced with *F*, which is the resultant force of *F1* and *F2*. The MC of the microelements from tensile stress to compressive stress in different positions depends on the values of tangential tensile plastic deformation and radial compressive plastic deformation in each layer. The former is proportional to the radius, while the latter is inversely proportional to the radius.
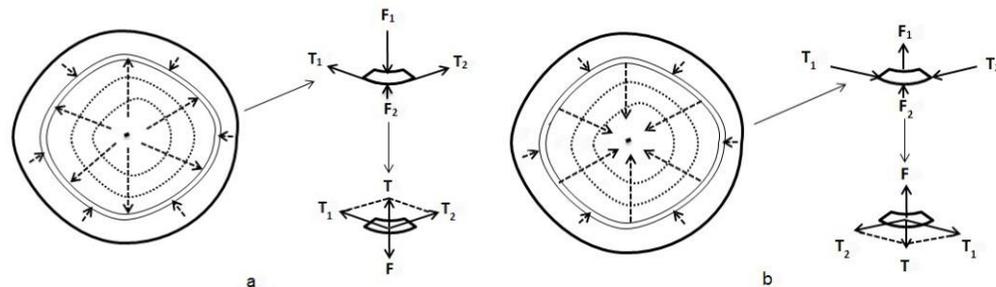

Fig. 4. Diagram of stress analysis in wood disks

RESULTS AND DISCUSSION

The Variation of Elastic Strain Characteristics

The radial distribution of elastic strain at different MCs is depicted in Fig. 5. At 26% MC, the main strain was a tangential tensile elastic strain that appeared to be a tangential tensile stress. At 18% MC, the tensile strain was completely replaced by the compressive strain; at this time, a compressive stress corresponded to the strain. The reason for this change at 26% MC, is that tangential tensile strain is caused by the differences in radial shrinkage with a small shrinkage ratio and tangential shrinkage with a large shrinkage ratio; stress reversal from tangential tensile stress to compressive stress is caused by the tensile plastic deformation produced previously.

From Fig. 5, it can be speculated that the stress reversal occurred between 26% MC and 18% MC. The elastic strain decreased gradually with decreasing MC; this might be due to the fact that the elastic modulus increased with decreasing MC below the FSP (Tu *et al*. 2007), but the primary reason was stress relaxation caused by creep. At different MC levels, elastic strain increased gradually from the pith toward the bark; at a distance of 50 mm from the pith, elastic strain decreased to some degree, and it was stable near the bark.
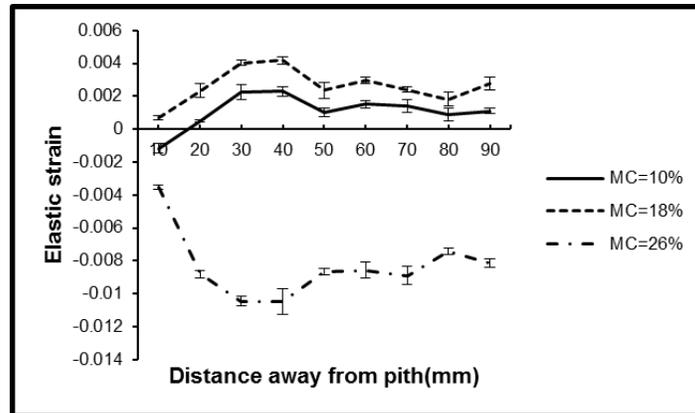
Fig. 5. The radial distribution of elastic strain at different MCs

The Variation of Viscoelastic Creep Strain Characteristics

Wood, as a natural polymer material, shows the viscoelastic properties of polymer materials, leading to a gradual recovery over time when the stress is released or reversed. Viscoelastic creep strain variation from pith to bark at different MCs is depicted in Fig. 6. The viscoelastic creep strain increased with increasing MC. As increasing water reduces the internal friction coefficient in the wood, additionally hygroscopic water in the cell wall provides good lubrication, making the wood flow easily even in the solid state (Dai and Liang 1987). At 26% MC, tensile viscoelastic creep appeared under tensile stress, and the creep near the pith was higher than it was close to the bark, indicating that the duration of tensile stress is longer near the pith. At 18% MC, all parts of the wood disk were subjected to compressive stress, but the strain was still a tensile strain, indicating that the stress reversal time was short and the tensile viscoelastic creep did not recover fully. At 10% MC, under compressive stress, only a small part of viscoelastic creep strain was transformed to a compressive strain because of the abnormal material properties, maybe it was the border between sapwood and heartwood; the other parts were still under a tensile strain, but with a value close to 0. As shown in Fig. 6, there were little variations of creep value at different MCs near the bark, indicating that it was difficult for the viscoelastic creep strain to emerge and recover at this position. The abnormalities of viscoelastic creep strain all appeared at 30 mm from the pith at different MCs.
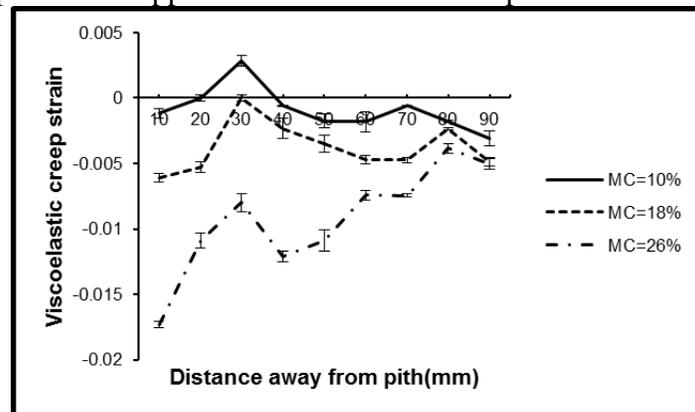

Fig. 6. The radial distribution of viscoelastic creep strain at different MCs

The Characteristics of MS Creep Strain Variation

MS creep strain is a permanent deformation that occurs with changes in temperature and MC. It is associated with wood properties, internal stress, MC, and temperature. It can also reduce the interaction of layers inside timber (Pang 2000). The distribution of MS creep strain from pith to bark at different MCs is depicted in Fig. 7. At 26% MC, the heartwood underwent a tensile plastic deformation under the effect of tensile stress, but the sapwood area did not show this phenomenon, presumably because tensile stress in sapwood is small and less than the limit of proportionality. At 18% MC, the overall strain was exhibited as compressive MC strain. This is related to the differences in material performance, such as earlywood and latewood or heartwood and sapwood. When MC is 26%, only locally-produced tangential tensile plastic deformation was present. After stress reversal, part of the deformation gradually recovered and even produced anti-deformation, while other parts produced greater tangential compressive deformation; thus, the overall strain was compressive MC strain. At 10% MC, under the effect of continuous compressive stress, compressive plastic deformation occurred gradually, with the strain increasing accordingly. In general, MS creep strain increased with decreasing MC. When the MCs were 10% and 18%, MS creep strain increased from pith to bark.
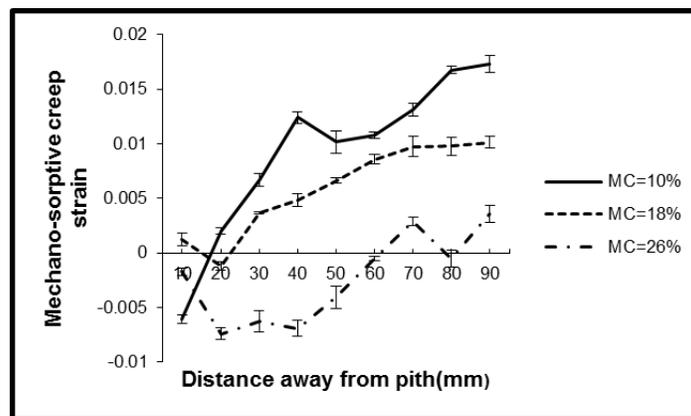

Fig. 7. The radial distribution of MS creep strain at different MCs

Inference

Viscoelastic creep strain and MS creep strain develop during slow drying due to the existence of shrinkage anisotropy, internal stress, and elastic strain, even if the moisture is uniformly distributed. Despite the fact that the strain value is not large compared to the shrinkage strain, it will produce cracks and deformation when no effective measures are taken during drying or application. Separate measurement and analysis of the strain caused by shrinkage anisotropy were used to prepare a follow-up study into the mechanisms of the combined action by MC gradient and shrinkage anisotropy. A better understanding of the interaction between MC gradient and shrinkage anisotropy might be useful in minimizing drying stress to achieve the goal of drying safely.

CONCLUSIONS

1. Below the FSP, the wood disks are initially subject to tangential tensile stress. With decreasing MC, the tensile stress turns into a compressive stress.

2. All strains were closely related to the MC. MS creep strain increased with decreasing MC, while elastic strain and viscoelastic creep were positively correlated with MC.

3. Each strain showed different changes from pith to bark; elastic strain decreased after first increasing and then remained stable. The abnormalities of viscoelastic creep strain all appeared at 30 mm from the pith, and there were little variations of creep strain near the bark. MS creep strain increased at 10% MC and 18% MC from pith to bark.

4. During the drying of wood disks, the internal stress produced by drying shrinkage anisotropy is unavoidable and it is one of the main factors causing cracks in the drying process or application.

5. In further studies, it is necessary to investigate each strain caused by the interaction between MC gradient and shrinkage anisotropy during drying. Such information will provide the theoretical basis for using rheology theory to interpret an inhibitive mechanism of cracks.

ACKNOWLEDGMENTS

REFERENCES CITED

Armstrong, L. D., Kingston, R. S. T. (1960). "Effect of moisture changes on creep in wood," *Nature* 185(4716), 862-863.

Armstrong, L. D., Kingston, R. S. T. (1962). "The effect of moisture content on the deformation of wood under stress," *Austr. J. Appl. Sci.* 13(4), 257-276.

Ai, M. Y., Zhang, X. F., Zhu, Z. X., Li, Y. J., and Chen, G. Y. (1996). "Study on drying technology for wood disc from small diameter Asian white birch," *China Wood Industry* 10(3), 13-15.

Bergman, R. (2010). "Drying and control of moisture content and dimensional changes," *Wood Handbook*, Madison, WI: U.S. Department of Agriculture, Forest Service, Forest Products Laboratory, Chapter13-7.

Dai, C. Y., and Liang, B. H. (1987). "Viscoelastic properties of wood under long-term load," *Journal of Northeast Forestry University* 15(5), 53-60.

Erickson, R. W., and Seavey, R. T. (1992). "Energy quantification and mechano-sorptive behavior in the kiln drying of 2.5 cm thick red oak lumber," *Drying Technology* 10(5), 1183-1206.

Hunt, D. G. (1989). "Linearity and non-linearity in mechano-sorptive creep of softwood in compression and bending," *Wood Sci. Technol*. 22,199-210.

Hasalania, M., and Itayaa, Y. (1996). "Drying-induced strain and stress: A review," *Drying Technology* 14(5), 1011-1040.

Kang, W., and Lee, N.-H. (2004). "Relationship between radial variations in shrinkage and drying defects of tree disks," *Journal of Wood Science* 50(3), 209-216.

Lee, N.-H., and Hayashi, K. (2000). "Effect of end-covering and low pressure steam explosion treatment on drying rate and checking during radio-frequency/vacuum drying of Japanese cedar log cross sections," *Forest Prod. J* 50(2), 73-78.

Li, D. G., and Gu, L. B. (1999). "Study on rheological behaviour of surface layer of poplar during high-temperature drying," *Scientia Silvae Sinicae* 35(1), 83-89.

McMillen, J. M. (1955a). "Drying stress in red oak," *Forest Products Journal* 5(2), 71-76.

McMillen, J. M. (1955b). "Drying stress in red oak," *Forest Products Journal* 5(4), 230-241.

Pang, S. (2000). "Modelling of stress development during drying and relief during steaming in *Pinus radiata* lumber," *Drying Technology* 18(8), 1677-1696.

Rice, R. W., and Youngs, R. L. (1990). "The mechanism and development of creep during drying of red oak," *Holz Roh Werkst*. 48(1), 73-79.

Svensson, S. (1995) "Strain and shrinkage force in wood under kiln drying conditions. 1. Measuring strain and shrinkage under controlled climate conditions - Equipment and preliminary results," *Holzforschung* 49(4), 363-368.

Svensson, S. (1996) "Strain and shrinkage force in wood under kiln drying conditions. 2. Strain, shrinkage and stress measurements under controlled climate conditions," *Holzforschung* 50(5), 463-469.

Tu, D. Y., Gu, L. B., Liu, B., and Zhou, X. (2007). "Modeling and on-line measurement of drying stress of *Pinus massoniana* board," *Drying Technology* 25(3), 441-448.

Ugolev, B. N. (1976). "General laws of wood deformation and rheological properties of hardwood," *Wood Science and Technology* 10, 169-181.

Wang, X. M., Gao, Z. Y., An, Z., and Meng, L. P. (1997). "Study on drying characteristics of small diameter birch discs modified with urea and UF resin," *China Wood Industry* 12(1), 14-25.

Yang, L. Q. (2011). "The research of preprocessing and drying characteristics of *B.costata* disk," *Northeast Forestry University*, Harbin, 12-13.

Zhan, J. F., Gu, J. Y., and Ai, M. Y. (2004). "The preliminary study on drying process traverse strains of Asian white birch," *Scientia Silvae Sinicae* 40(5), 174-179

Zhan, J. F., Gu, J. Y., and Shi, S. Q. (2009). "Rheological behavior of larch timber during conventional drying," *Drying Technology* 27(10), 1041-1050.